A Distributed Double-Newton Descent Algorithm for Cooperative Energy Management of Multiple Energy Bodies in Energy Internet

Yushuai Li, *Member, IEEE*, David Wenzhong Gao, *Senior Member, IEEE*, Wei Gao, *Graduate Student Member, IEEE*, Huaguang Zhang, *Fellow, IEEE*, and Jianguo Zhou, *Member, IEEE*

***Abstract*—This article investigates the problem of distributed cooperative energy management of multiple energy bodies with the consideration of both the optimal energy generation/consumption of each participant within single energy body and the optimal energy distribution on the interconnected lines between any pair of energy bodies. First, we define the physical and communication structure of the system formed by many energy bodies, each of which is viewed as a multienergy prosumer. Then, a distributed energy management model is proposed to achieve not only maximum profits of overall energy generation and consumption, but also minimum cost of energy delivery. To address this issue, a distributed double-Newton descent (DDND) algorithm is proposed, which possesses two advantages. On the one hand, by employing second-order information, the concept of Newton descent is embedded into the implementation of the proposed algorithm, resulting in faster convergence speed. On the other hand, the proposed algorithm performs in a fully distributed fashion. As a consequence, each participant can locally obtain its optimal operation as well as the global energy market clearing prices; meanwhile, each energy router can locally obtain the optimal exchanged energy with its neighbor energy routers. Moreover, we prove that the proposed DDND algorithm can asymptotically converge to the global optimal point. As a result, the correctness of the DDND algorithm can be guaranteed in theory. Finally, simulation results validate the effectiveness of the proposed algorithm.**

***Index Terms*—Distributed algorithm, energy body (EB), energy internet (EI), Newton descent.**

Manuscript received May 28, 2020; revised August 21, 2020 and October 5, 2020; accepted October 7, 2020. Date of publication October 12, 2020; date of current version June 16, 2021. This work was supported by the U.S. National Science Foundation under Grant 1711951. Paper no. TII-20-2655. *(Corresponding author: David Wenzhong Gao.)*

Yushuai Li is with the School of Information Science and Engineering, Northeastern University, Shenyang 110004, China, and also with the Department of Electrical and Computer Engineering, University of Denver, Denver, CO 80208 USA (e-mail: yushuaili@ieee.org).

David Wenzhong Gao and Wei Gao are with the Department of Electrical and Computer Engineering, University of Denver, Denver, CO 80208 USA (e-mail: Wenzhong.Gao@du.edu; wei.gao@du.edu).

Huaguang Zhang is with the State Key Laboratory of Synthetical Automation for Process Industries (Northeastern University), Shenyang 110004, China, and also with the School of Information Science and Engineering, Northeastern University, Shenyang 110004, China (e-mail: hgzhang@ieee.org).

Jianguo Zhou is with the Tsinghua-Berkeley Shenzhen Institute (TBSI), Tsinghua Shenzhen International Graduate School (Tsinghua SIGS), Tsinghua University, 518055 Shenzhen, China (e-mail: JianguoZhou.NEU@gmail.com).

Color versions of one or more of the figures in this article are available online at https://ieeexplore.ieee.org.

Digital Object Identifier 10.1109/TII.2020.3029974

I. Introduction

As THE next-generation expansion of smart grid, the concept of energy internet (EI) is proposed and has gained wide attention in recent years [1]–[4]. Different from the smart grid, one important purpose of EI is to integrate multienergy networks (such as electricity grid, heat network, and gas network) and advanced communication technology to enhance system resilience, improve energy efficiency, and adopt higher penetration of renewable energy, etc. To achieve the smooth transition from smart grid to EI, the concept of energy body (EB) is proposed within the context of EI [5], which is analogous to the microgrid in smart electricity grid. However, different from the microgrid, the EB can effectively integrate different energy networks and simultaneously play multiple roles in energy production and consumption. This is because EB has inherent peer-to-peer functional relationship among different energy resources and is thus more suitable for EI model development. Since there exists strong-coupling among different energy networks, the energy management problem (EMP) is more complex and difficult in the aspects of modeling, algorithm design and theoretical analysis, etc., which necessitates to be studied to achieve the expected functionalities of EI.

The EMP is commonly viewed as an optimal decision problem with the objective of maximizing social welfare while meeting load demands and a set of operation constraints. Up to the present, significant amount of work have been done on this topic within the context of smart grid or EI. Generally, the approaches to search for the global optimal operations can be roughly grouped into two categories, i.e., centralized method and distributed method. Note that the centralized method depends on powerful centralized controller and two-way communication structure which may incur higher computation cost, and suffer from single-point failures and weak privacy. To overcome these deficiencies, the distributed method mainly focuses on disaggregating the global computation problem and assigning to individual and distributed energy device, which only utilizes local information and computation to obtain the optimal operation, leading to better robustness [6], scalability [7], flexibility [8], and privacy [9], [10], etc. Now, the distributed method has become the most important analysis method and been seen as a promising alternative. Chow *et al.* [11] first introduced the incremental consensus algorithm to smart grid in, which can solve the economic dispatch problem in a distributed fashion. Since this method requires a leader agent, it cannot be seen as a fully distributed method. To solve the economic dispatch problem in a fully distributed manner, the Lambda-Iteration based method was proposed in [12]. On the basis of [12], Xu *et al.* [13] first proposed a fully distributed control strategy to solve the EMP considering the impact of the component level response. Therein, the upper control level is designed to obtain the optimal power generation/demand which is further used as power reference for the associated component in lower control level. Note that the considered cost function in [11]–[13] are quadratic-form. The designed distributed algorithm and theoretical analysis method are mainly suitable for quadratic-form optimization. In this article, we will consider more complex cost function and design more universal distributed algorithm. Many distributed energy management strategies have been presented thereafter under this background. Therein, the major concerns include the effects of communication delays [14], [15], nonconvex analysis [16], [17], underlying control [18], [19], and network attacks [20], [21], etc.

Of note, the above research mainly focuses on solving the EMP for power system without considering the interdependence and co-planning of different energy systems. To address this issue, Zhang *et al.* [5] defined an energy management framework for EI with multi-EB and analyzed its structure as well as benefits, which extends the EMP from smart grid to EI. Therein, a distributed-consensus-ADMM was proposed, which can effectively handle the power-heat-gas coupling problem during energy generation and consumption. Under this framework, the multitimescale energy management model was further built in [22], where an event-triggered based method was proposed to solve the EMP. Later, similar to EB, the concept of We-Energy was presented in [23]. However, the considered cost model for each energy device is of quadratic-form; meanwhile, the proposed double-consensus algorithm is only suitable for quadratic-form optimization, which makes it not suitable for EI with complex cost functions and constrains. In [24], a neurodynamics-based algorithm was proposed and applied to solve the EMP in multienergy system.

The previous work have better modeled the different coupling modes among different energy networks and developed multiple distributed algorithms to focus only on the local optimal energy generation and consumption. However, the planning of the energy distribution on the interconnected power line, heat pipeline, and gas pipeline among EBs are not considered. Although some constraints of the power line and heat pipeline were taken into account in [25], the optimal allocation of exchanged power, heat, and gas on interconnected lines was not addressed. Under interconnected mode of multi-EB, the optimal energy distribution among EBs is very important and the reasons are as follows.

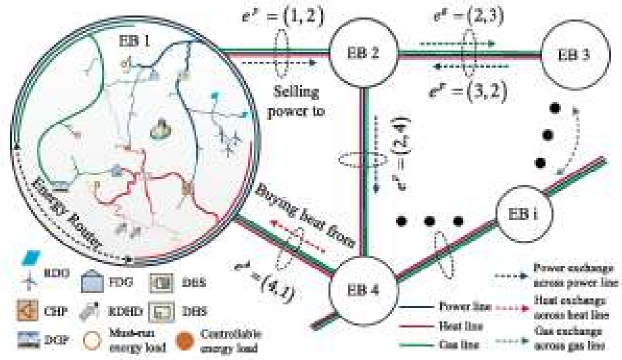

Fig. 1. Physical structure of interlinked multi-EBs.

First, each EB is an independent individual. As seen in Fig. 1, each EB establishes physical connection and exchanges energy with only its neighbor EBs, but does not connect to a common energy bus. Thus, to complete the energy market transactions, each EB needs to know who and how much it should sell the excess energy to (or buy deficit energy from). Second, different EBs may have different structures. For instance, let us consider a pair of EBs connected with each other. With regard to the electricity element, the one EB may use ac network and the other may use dc network. Thus, as reference signals, the direction and amount of the exchanged power are both needed to control the underlying ac/dc or dc/ac converter to achieve the energy delivery. Last but not the least, different interconnected lines or pipelines may hold different properties such as distance and materials, etc., resulting in different energy delivery cost. Hence, the global planning of the optimal energy distribution will improve the economics and efficiency.

Up to now, few noticeable research has been documented to develop fully distributed algorithm based on local decision variables to simultaneously obtain the optimal energy generation/consumption for each distributed participant and the optimal energy distribution on interconnected lines within EI integrating multiple energy networks. The closest work that can be found is in [26]–[29] within multiarea or multimicrogrid scenario and in [25] within integrated energy system scenario. To be specific, the authors divided the node-branch sets into internal set and boundary set for each area in [26] and [27]. Each area only needs to share the information of each boundary set with neighbor areas to achieve collaborative economic dispatch. However, each area needs to collect all the information of its components. Although this method can achieve distributed calculation among multiareas, the internal implementation within single area is centralized. In [28], a distributed adjustable robust optimal scheduling algorithm is proposed to solve the collaborative EMP of multiple microgrids. Similar to [26] and [27], each microgrid also needs to centralizedly manage its internal components. In [29], the authors proposed a hierarchical energy management strategy to study the same problem as in [28]. However, under a tree-like structure, a centralized coordinator is needed to collect all the calculation results of microgrid subproblem as well as energy router (ER) subproblem, use them to calculate the optimal incremental cost, and then send back the optimal incremental cost to each microgrid and ER. The research in [26]–[29] have made some outstanding contributions to achieve the cooperative management of multimicrogrids. Nevertheless, the coordinator is also needed to either manage internal participants of individual microgrid [26]–[28], or calculate part of global variables [29]. This also means that the global computation processes are not fully divided and assigned to distributed participants or energy devices, resulting in not fully distributed implementation. In this article, we would like to find the optimal energy generation/consumption for each distributed participant and the optimal energy distribution on interconnected lines in a fully distributed fashion. Thus, the methods proposed in [26]–[29] cannot be used to solve our studied problem. In addition, the studied problem in [26]–[29] is for multiple electricity microgrids without the consideration of the interaction of different energy networks. Based on the neurodynamic algorithm [30], a distributed optimization approach was proposed to solve the economic dispatch problem for integrated energy system in [25]. It is worth noting that the research in [25] has done outstanding contributions to achieve the cooperated operation for integrated electricity and heat network considering the transmission power line and heat pipeline congestions. However, like the method in [30], the decision variables (i.e., the variables needed to be calculated) for each agent in [25] are composed of all the variables of the whole system (i.e., the global variables) during the algorithm implementation. The decision variables for each agent will finally converge to the same values which are the optimal solutions for the global variables. In this article, we hope that the decision variables of each agent (i.e., participant or ER) only include its local variables. Thus, the distributed methods proposed in [25] and [30] are not suitable for our work.

To address those challenges, we try to propose distributed model and method to find the optimal energy generation/consumption for distributed participants as well as the optimal energy distribution on interconnected lines in a fully distributed fashion based on local decision variables within the concept of EB-based EI. The major contributions of this article are summarized as follows.

1) A fully distributed model for multiobjective EMP, integrating the planning of optimal energy generation/consumption for internal participants within each EB and external energy distribution on interconnected edges between any pair of EBs, is presented in this article. The studied problem is further formulated as a distributed optimization problem involving many different kinds of coupled equality and inequality constraints. Therein, each participant or ER only needs to know it local decision variables.

2) A distributed double-Newton descent (DDND) algorithm is proposed to find the global optimal solution of the studied problem. Compared with the literature [26]–[29], the proposed algorithm can be implemented in a fully distributed manner without needing any coordinator. Compared with [25] and [30], the proposed algorithm enables each participant or ER only needing to know its local variables and sharing several low-dimensional auxiliary variables with its neighbors to obtain the local optimal operations. To the authors' best knowledge, it is the first time to simultaneously obtain the optimal operation for individual participant and the optimal energy distribution among EBs in a fully distributed manner by only using local decision variables for EB-based EI.

3) The Newton descent concept is uniquely embedded into the execution of the proposed algorithm. Due to the utilization of second-order information, the convergence speed of our distributed algorithm is greatly improved when compared with the distributed gradient-based descent method.

4) One Lemma and two Theorems are presented to prove the feasibility of the proposed algorithm. Based on those theoretical analysis, we can conclude that the proposed algorithm can converge to the global optimal solution.

II. System Structure and Preliminary Formulation

A possible layout of interlinked EBs is shown in Fig. 1, where each EB is equipped with an ER to control the energy exchange with other interconnected EBs. As both energy supplier and consumer, each EB integrates multiple energy resources, including various types of renewable distributed generators (RDGs), fuel-based distributed generators (FDGs), renewable distributed heating devices (RDHDs), fuel-based distributed heating devices (FDHDs), distributed combined heat and power (DCHPs) devices, distributed electricity storages (DESs), distributed heat storages (DHSs), and distributed gas providers (DGPs). Additionally, we consider three types of energy loads, i.e., power, heat and gas loads, each of which contains an equivalent must-run load and a controllable load. Each EB can operate in island-mode or interconnected mode by exchanging energy with neighbor EBs via the linked lines. In terms of different application scenarios, the EB can be regarded as small as a residential house or as large as a town.

A. EB Model

With regard to the internal energy generations/consumptions in individual EB, the electricity power generations come from the RDG, FDG, and DCHP, denoted as p_i^{re}, p_i^{fu}, and p_i^{chp}, respectively. The heat generations come from the RDHD, FDHD, and DCHP, denoted as h_i^{re}, h_i^{fu}, and h_i^{chp}, respectively. The gas is fed by the DGP denoted as g_i^{gas}. Based on the charging and discharging states, the DES and DHS can act at energy supplier or consumer. We denote p_i^{st} and h_i^{st} as the exchanged power and heat for DES and DHS, respectively; meanwhile, we let p_i^{st} or h_i^{st} be positive for discharging and negative for charging. For the energy loads, $l_i^{p,m}$ (or $l_i^{p,c}$), $l_i^{h,m}$ (or $l_i^{h,c}$), and $l_i^{g,m}$ (or $l_i^{g,c}$) are employed to represent the must-run (or controllable) power, must-run (or controllable) heat, and must-run (or controllable) gas loads, respectively. Stimulated by the profit, each EB is able to simultaneously take the rule energy supplier and consumer by managing its internal participants. We let p_i^{im}, h_i^{im}, and g_i^{im} represent the imbalance (deficit or overabundance) power, heat, and gas. The energy balance constraints for ith EB at time T are given by

$$p_{i,T}^{im} = p_{i,T}^{re} + p_{i,T}^{fu} + p_{i,T}^{chp} + p_{i,T}^{st} - l_{i,T}^{p,m} - l_{i,T}^{p,c}; \qquad (1)$$

$$h_{i,T}^{tm} = h_{i,T}^{re} + h_{i,T}^{fu} + h_{i,T}^{chp} + h_{i,T}^{st} - l_{i,T}^{h,m} - l_{i,T}^{h,c}; \quad (2)$$

$$g_{i,T}^{tm} = g_{i,T}^{\text{gas}} - l_{i,T}^{g,m} - l_{i,T}^{g,c}. \quad (3)$$

Apart from the supply demand balance constrains, each EB is limited to a set of local operation constraints mainly containing the following six types.

1) The capability constraints for FDG, FDHD, and DGP

$$\psi_i^{fu,\min} \le \psi_{i,T}^{fu} \le \psi_i^{fu,\max}; \qquad \psi \in p, h \quad (4)$$

$$0 \le g_i^{\text{gas,min}} \le g_{i,T}^{\text{gas}} \le g_i^{\text{gas,max}} \quad (5)$$

where superscript "min" and "max" represent the corresponding minimum and maximum allowed bounds, and symbol ψ is used to represent p or h (i.e., the variables related to power or heat) to simplify notations.

2) Confidence constraints with the consideration of forecasting errors for RDG and RDHD [5]

$$\psi_{i,T}^{re,\min} \le \psi_{i,T}^{re} \le \psi_{i,T}^{re,\max}. \qquad \psi \in p, h \quad (6)$$

3) The feasible operation region for DCHP

$$\vartheta_{i,\kappa}^1 p_{i,T}^{chp} + \vartheta_{i,\kappa}^2 h_{i,T}^{chp} + \vartheta_{i,\kappa}^3 \ge 0, \quad \kappa = 1,2,3,4 \quad (7)$$

where $\vartheta_{i,\kappa}^1$, $\vartheta_{i,\kappa}^2$, and $\vartheta_{i,\kappa}^3$ are coefficients of κth linear inequality constraint [23].

4) The ramp rate limits for FDG and DCHP

$$-p_i^{fu,\text{ramp}} \le p_{i,T}^{fu} - p_{i,T-1}^{fu} \le p_i^{fu,\text{ramp}} \quad (8)$$

$$-p_i^{chp,\text{ramp}} \le p_{i,T}^{chp} - p_{i,T-1}^{chp} \le p_i^{chp,\text{ramp}} \quad (9)$$

where $p_{i,T}^{fu,\text{ramp}}$ and $p_{i,T}^{chp,\text{ramp}}$ are the ramp rates.

5) The feasible charging/discharging actions and stored energy for DES and DHS [31]

$$-\psi_i^{ch,\max} \le \psi_{i,T}^{st} \le \psi_i^{ds,\max}; \qquad \psi \in p, h \quad (10)$$

$$SOC_{i,T}^{\psi} = SOC_{i,T-1}^{\psi} - \psi_{i,T-1}^{st}\Delta T; \qquad \psi \in p, h \quad (11)$$

$$SOC_i^{\psi,\min} \le SOC_{i,T}^{\psi} \le SOC_i^{\psi,\max}, \qquad \psi \in p, h \quad (12)$$

where $\psi_i^{ch,\max}$ and $\psi_i^{ds,\max}$ are the maximum charging and discharging rates, respectively; $SOC_{i,T}^{\psi}$ is state of charge (the stored energy).

6) Energy loads constraints and relevant ratios of energy loads [5]

$$0 \le l_{i,T}^{p,c} \le l_{i,T}^{p,\max} - l_{i,T}^{p,m}; \quad (13)$$

$$0 \le l_{i,T}^{h,c} \le l_{i,T}^{h,\max} - l_{i,T}^{h,m}; \quad (14)$$

$$0 \le l_{i,T}^{g,c} \le l_{i,T}^{g,\max} - l_{i,T}^{g,m}; \quad (15)$$

$$\Upsilon_{i,g\to p}^{\min} \le l_{i,T}^{p,c}/(l_{i,T}^{p,c} + \Psi l_{i,T}^{g,c}) \le \Upsilon_{i,g\to p}^{\max}; \quad (16)$$

$$\Upsilon_{i,g\to h}^{\min} \le l_{i,T}^{h,c}/(l_{i,T}^{h,c} + \Psi l_{i,T}^{g,c}) \le \Upsilon_{i,g\to h}^{\max}; \quad (17)$$

$$\Upsilon_{i,h\to p}^{\min} \le l_{i,T}^{p,c}/(l_{i,T}^{p,c} + l_{i,T}^{h,c}) \le \Upsilon_{i,h\to p}^{\min} \quad (18)$$

where $\Upsilon_{i,g\to p}$, $\Upsilon_{i,g\to h}$, and $\Upsilon_{i,h\to p}$ refer to the ratio of electric power load with respect to combined power and gas load, the ratio of heat load with respect to combined heat and gas load, and the ratio of electric power load with respect to combined power and heat load, respectively. Ψ is the conversion ratio from SCM/h (gas flow rate) to MW and its value is often set to $1/84$.

The benefit function for individual EB used to guide the optimal operation behavior consists of the following six parts

1) The cost functions of FDG and FDHD, i.e., (19), and DCHP, i.e., (20), derived from the fuel cost are

$$C(\psi_{i,T}^{fu}) = a_i^{\psi,fu}(\psi_{i,T}^{fu})^2 + b_i^{\psi,fu}\psi_{i,T}^{fu} + c_i^{\psi,fu} + \varepsilon_i^{\psi,fu}\exp(\xi_i^{\psi,fu}\psi_{i,T}^{fu}); \quad (19)$$

$$C(p_{i,T}^{chp}, h_{i,T}^{chp}) = a_i^{chp}(p_{i,T}^{chp})^2 + b_i^{chp}p_{i,T}^{chp} + d_i^{chp}p_{i,T}^{chp}h_{i,T}^{chp} + e_i^{chp}(h_{i,T}^{chp})^2 + f_i^{chp}h_{i,T}^{chp} + c_i^{chp} \quad (20)$$

where $a_i^{\psi,fu}$, $b_i^{\psi,fu}$, $c_i^{\psi,fu}$, $\varepsilon_i^{\psi,fu}$, $\xi_i^{\psi,fu}$, a_i^{chp}, b_i^{chp}, $d_i^{chp}e_i^{chp}$, f_i^{chp}, c_i^{chp} represent nonnegative cost coefficients.

2) The cost functions of RDG and RDHD with the consideration of the tradeoff between the optimality and generation possibility are [5]

$$C(\psi_{i,T}^{re}) = a_i^{\psi,re}\psi_{i,T}^{re} + b_i^{\psi,re}\exp\left(\xi_i^{\psi,re}\frac{\psi_{i,T}^{re,\max} - \psi_{i,T}^{re}}{\psi_{i,T}^{re,\max} - \psi_{i,T}^{re,\min}}\right) \quad (21)$$

where $a_i^{\psi,re}$ and $b_i^{\psi,re}$ are nonnegative cost coefficients; $\xi_i^{\psi,re}$ is the penalty coefficient.

3) The cost functions of DES and DHS are [28]

$$C(\psi_{i,T}^{st}) = a_i^{\psi,st}(\psi_{i,T}^{st} + b_i^{\psi,st})^2 \quad (22)$$

where $a_i^{\psi,st}$ and $b_i^{\psi,st}$ are cost coefficients.

4) The cost function of DGP is [5]

$$C(g_{i,T}^{\text{gas}}) = a_i^g(g_{i,T}^{\text{gas}})^3 + b_i^g(g_{i,T}^{\text{gas}})^2 + d_i^g g_{i,T}^{\text{gas}} + c_i^g \quad (23)$$

where a_i^g, b_i^g, d_i^g, and c_i^g are nonnegative cost coefficients. In addition, it should be pointed out that $C(g_{i,T}^{\text{gas}})$ is convex within the constraint (5).

5) The utility function for energy loads with the consideration of demand response is

$$U(l_{i,T}^{p,c}, l_{i,T}^{h,c}, l_{i,T}^{g,c}) = -\alpha_i^p(l_{i,T}^{p,m} + l_{i,T}^{p,c})^2 + \beta_i^p(l_{i,T}^{p,m} + l_{i,T}^{p,c}) - \alpha_i^h(l_{i,T}^{h,m} + l_{i,T}^{h,c})^2 + \beta_i^h(l_{i,T}^{h,m} + l_{i,T}^{h,c}) - \alpha_i^g(l_{i,T}^{g,m} + l_{i,T}^{g,c})^2 + \beta_i^g(l_{i,T}^{g,m} + l_{i,T}^{g,c}) \quad (24)$$

where α_i^p, β_i^p, α_i^h, β_i^h, α_i^g, and β_i^g are nonnegative utility coefficients.

6) The income (cost) for selling (purchasing) energy to (from) other EB(s) is

$$UC_{i,T} = pri_{i,T}^p p_{i,T}^{tm} + pri_{i,T}^h h_{i,T}^{tm} + pri_{i,T}^g g_{i,T}^{tm} \quad (25)$$

where $pri_{i,T}^p$, $pri_{i,T}^h$, and $pri_{i,T}^g$ are the market clearing prices for power, heat, and gas, respectively.

B. Energy Distribution Model Among EBs

By controlling the local ER as seen in Fig. 1, each EB can sell surplus energy to other EBs to make additional profits and/or purchase deficit energy from other EBs to meet its internal energy demands. The energy distribution can be modeled as the representation of graph structure. We define three energy distribution graphs corresponding to the different physical links of power, heat, and gas among EBs. First, a power distribution graph is defined as $\mathcal{G}^p = (\mathcal{N}, \mathcal{E}^p, O^p)$, where $\mathcal{N} = \{1, 2, \cdots, n\}$ is the set of nodes representing all the ERs, $\mathcal{E}^p = \{1, 2, \cdots, E^p\}$ is the set of edges representing the power exchange across the corresponding interconnected power line, and $O^p = \{o_{i,e^p}\}$ is node-edge incidence matrix. Therein, $i \in \mathcal{N}, e^p \in \mathcal{E}^p; o_{i,e^p} = 1$ if edge leaves node i; $o_{i,e^p} = -1$ if edge enters node i; $o_{i,e^p} = 0$, otherwise. The amount of power exchange on edge $e^p = (i, k)$ is defined as χ_{e^p}. The delivery cost function is used to guide the system power distribution, which can be modeled as [29]

$$C(\chi_{e^p}) = a_e^p (\chi_{e^p})^2 \tag{26}$$

where $a_e^p > 0$ is the cost coefficient. Moreover, if the final calculation result of $\chi_{e^p} \geq 0$, it means that the final power exchange across edge $e^p = (i, k)$ is from node i to node k; Otherwise (i.e., $\chi_{e^p} < 0$), it means that the final power exchange across edge $e^p = (i, k)$ is from node k to node i. The maximum power transmission capability on $e^p = (i, k)$ is defined as $\chi_{e^p}^{\max}$, such that

$$-\chi_{e^p}^{\max} \leq \chi_{e^p} \leq \chi_{e^p}^{\max} \tag{27}$$

where (27) represents the transmission line congestion constraint.

Now, node i can be seen as a source node with outgoing rate $p_{i,T}^{tm}$ if $p_{i,T}^{tm} > 0$; otherwise, it is seen as a sink node with incoming rate $p_{i,T}^{tm} <= 0$. Then, the node-edge (or node-branch) power flow balance constraint is modeled as

$$O^p \chi^p = p^{tm} \tag{28}$$

where χ^p and p^{tm} are the column vector forms of χ_{e^p} and $p_{i,T}^{tm}$, respectively. In addition, caused by the system total power supply-demand balance, the total values of incoming power are equal to the ones of outgoing power, i.e., $\sum_{i=1}^{n} p_{i,T}^{tm} = 0$.

Based on the aforementioned model, the problem of finding the optimal power distribution among EBs can be formulated as a kind of dynamic network flow optimization problem with multiple source and sink nodes. In the subsequent algorithm design part, we will provide its distributed solution. Moreover, the Algebraic connectivity of $\mathcal{G}^p$ is determined by the second smallest eigenvalue of graph Laplacian $O^p O^{pT}$. To ensure solutions feasibility, we assume $\mathcal{G}^P$ is connected. It also means that $O^p O^{pT}$ is symmetric, singular and positive semidefinite.

The similar definition and model of power distribution can be applied for heat distribution and gas distribution. We let $\mathcal{G}^h = (\mathcal{N}, \mathcal{E}^h, O^h)$ and $\mathcal{G}^g = (\mathcal{N}, \mathcal{E}^g, O^g)$ represent the heat and gas distribution graphs, respectively, where $\mathcal{E}^h = \{1, 2, \cdots, E^h\}$, $\mathcal{E}^g = \{1, 2, \cdots, E^g\}$, $O_{i,e^h} = \{o_{i,e^h}\}$, and $O_{i,e^h} = \{o_{i,e^g}\}$. $C(\chi_{e^h})$ and $C(\chi_{e^g})$ are denoted as the corresponding delivery cost functions for χ_{e^h} and χ_{e^g}, respectively. $\chi_{e^h}^{\max}$ and $\chi_{e^g}^{\max}$ are the maximum heat and gas transmission capability on edges e^h and e^g, respectively. The node-edge heat flow and gas flow balance constraints as well as the heat and gas pipeline congestion constraints should also be fulfilled, i.e.,

$$O^h \chi^h = h^{tm}; -\chi_{e^h}^{\max} \leq \chi_{e^h} \leq \chi_{e^h}^{\max}; \tag{29}$$

$$O^g \chi^g = g^{tm}; -\chi_{e^g}^{\max} \leq \chi_{e^g} \leq \chi_{e^g}^{\max}. \tag{30}$$

C. Multiobjective Energy Management of EBs

We consider an EI system with n EBs; meanwhile, EB i has m_i participants (i.e., RDG, FDG, RDHD, DCHP, DES, DGP, and schedulable energy loads, etc.). The objective is to find the optimal operations with maximum social welfare (sw) of EBs and optimal energy distribution with minimum delivery costs (dc) among EBs, which is defined as follows:

$$\max \quad \text{Obj} = \sum_{i=1}^{n} F_{i,T}^{\text{sw}} - F_{i,T}^{dc} \tag{31}$$

with

$$F_{i,T}^{\text{sw}} = -\sum_{\psi \in p,h} \left(C(\psi_{i,T}^{fu}) + C(\psi_{i,T}^{re}) + C(\psi_{i,T}^{st}) \right) - C(g_{i,T}^{\text{gas}})$$
$$- C(p_{i,T}^{chp}, h_{i,T}^{chp}) + U(l_{i,T}^{p,c}, l_{i,T}^{h,c}, l_{i,T}^{g,c}) + UC_{i,T}$$

$$F_{i,T}^{dc} = \sum_{e^p=1}^{E^p} C(\chi_{e^p}) + \sum_{e^h=1}^{E^h} C(\chi_{e^h}) + \sum_{e^g=1}^{E^g} C(\chi_{e^g})$$

subject to

$$\sum_{i=1}^{n} p_{i,T}^{tm} = 0; \sum_{i=1}^{n} h_{i,T}^{tm} = 0; \sum_{i=1}^{n} g_{i,T}^{tm} = 0 \tag{32}$$

and (4)–(18), (27)–(30).

Next, to simplify notations, we define that $x_{ij} \in \mathrm{R}^3$ is a 3-D vector composed of the power, heat and gas of the jth participant of ith EB. Note that some of those elements may be zero(s) depending on the characteristics of the participant. We also define that $l_{ij}^m \in \mathrm{R}^3$ is a 3-D vector composed of the power, heat and gas of the jth must-run energy loads of ith EB. Each participant is able to transform its variable to the form of x_{ij} by making the upper and lower bounds of each zero(s) variable be zeros; meanwhile, the cost function(s) corresponding to the zero variable(s) is(are) set to any kind of strongly convex function(s) like that defined in (19). In addition, the ER plays the role of exchanging energy as well as information with other ERs. To estimate the value of exchanged energy, i.e., $p_{i,T}^{tm}$, $h_{i,T}^{tm}$, and $g_{i,T}^{tm}$, in a distributed energy network, we assign a dummy variable x_{ij} for the ER in ith EB and let $j = 0$. This is needed for later algorithm development such as in (40). Meanwhile, we also assign a strongly convex cost function for x_{i0} and let its bounds be zeros. Then, we let W_{ij} to represent the corresponding cost function or negative utility function. The above studied problem, as specified by (4)–(18), (27)–(32), can be rewritten as

$$\min \quad Obj = \sum_{i=1}^{n} \sum_{j=0}^{m_i} W(x_{ij}) + F_{i,T}^{dc} \tag{33}$$

subject to

$$\sum_{i=1}^{n}\sum_{j=0}^{m_i} B_{ij}x_{ij} = \sum_{i=1}^{n}\sum_{j=0}^{m_i} l_{ij}^{m}, \quad x_{ij} \in \Omega_{ij} \tag{34}$$

$$O^p\chi^p = p^{tm}; O^h\chi^h = h^{tm}; O^g\chi^g = g^{tm} \tag{35}$$

$$\chi_{e^p} \in \Omega_{e^p}; \chi_{e^h} \in \Omega_{e^h}; \chi_{e^g} \in \Omega_{e^g} \tag{36}$$

where $B_{ij} = -I_3$ if x_{ij} represents controllable energy load; otherwise, $B_{ij} = I_3$. Therein, I_3 is a 3-D identity matrix. Ω_{ij}, Ω_{e^p}, Ω_{e^h}, and Ω_{e^g} are the local closed convex sets determined by the local inequality constraints.

D. Analysis of Surface and Complexity

For an optimization problem, if the dimension of the decision variables is less than three, it is a good way to draw the objective function surface together with the constraint surface such that the global optimal point can be intuitively found. As a result, the optimization problem can be analyzed and solved in a better way. In our considered optimization problem (33)–(36), we focus on achieving the distributed cooperative energy management of multiple energy bodies with maximum total social welfare as well as minimum total delivery costs. We denote the system's total decision variables as $\mathrm{x} = [x_{ij=01}, \cdots, x_{ij=nm_i}, \chi_{e^p=1}, \cdots, \chi_{e^p=E^p}, \chi_{e^h=1}, \cdots, \chi_{e^h=E^h}, \chi_{e^g=1}, \cdots, \chi_{e^g=E^g}]$ which is the column vector made from concatenation of all x_{ij}, χ_{e^p}, χ_{e^h}, and χ_{e^g}. Therein, the variable for individual participant, i.e., x_{ij}, is 3-D, and the variable on each interconnected line, i.e., χ_{e^p} for power line, or χ_{e^h} for heat pipeline or χ_{e^g} for gas pipeline, is 1-D. Although the dimensions of x_{ij}, χ_{e^p}, χ_{e^h}, and χ_{e^g} are low, the overall decision variable vector x is high-dimensional in a large-scale EI with many participants and interconnected lines. Thus, the corresponding objective function surface is very complex. It is a difficult and even unrealistic task to draw the accurate objective function surface for the optimization problem with high-dimensional decision variables and also for problem (33)–(36). In this scenario, the graphical approach may not be viable. We have to use mathematical method to solve this problem. As we discussed in Appendix B in [32], our optimization function is strongly convex. Meanwhile, all the constraints are affine. Thus, the studied problem (33)–(36) is a typical convex optimization problem with only one global optimal solution.

Currently, many centralized mathematical approaches (such as the primal-dual interior-point (PDIP) approach) can be used to solve this kind of optimization problem. However, the centralized approach requires a centralized controller to collect all the information of each participant and interconnected lines in two-way communication structure. All the computation tasks have to be implemented in the centralized controller, which is subject to huge computing burden and cost as the EI system scale expands. In addition, the centralized approach also suffers from single-point failures and weak privacy, etc. To address these issues, this article designs distributed approach to find the global optimal solution, which further increases the complexity of the solution method. The complexity is reflected in how to disaggregate the global computation problem, and assign to individual participant and ER to respectively achieve the optimal operation and the energy distribution among EBs in a fully distributed fashion.

III. Newton-Based Distributed Energy Management Strategy

A. Distributed Communication Structure and Preliminary Knowledge

This article focuses on employing distributed communication manner to achieve local information sharing. The detailed design for the communication structures of single EB and their interconnections are presented in Appendix A in [32]. In addition, some basic knowledge of convex analysis, the definition of differentiated projection and a necessary Lemma (i.e., Lemma 1) are provided in Appendix B in [32], which is used for the subsequent convergence analysis.

B. Main Algorithm

In this section, we focus our attention on the exploration of fully distributed algorithm with faster convergence speed to solve problem (33) with constraints (34)–(36). The detailed design process of the proposed algorithm is presented in Appendix C in [32]. Based on the analysis in Appendix C in [32], the updating rules of the proposed algorithm are given by

$$\dot{x_{ij}} = \Gamma_{\Omega_{ij}}(\nabla^2 W(x_{ij})^{-1}x_{ij}, \nabla^2 W(x_{ij})^{-1}(-\nabla W(x_{ij}) + B_{ij}^T y_{ij})) \tag{37}$$

$$\dot{y_{ij}} = -\varpi \sum_{\overline{ij}\in N_{ij}} a_{ij,\overline{ij}}(y_{ij} - y_{\overline{ij}}) - \varpi \sum_{\overline{ij}\in N_{ij}} a_{ij,\overline{ij}}(z_{ij} - z_{\overline{ij}}) + l_{ij}^{m} - B_{ij}x_{ij} \tag{38}$$

$$\dot{z_{ij}} = \varpi \sum_{\overline{ij}\in N_{ij}} a_{ij,\overline{ij}}(y_{ij} - y_{\overline{ij}}) \tag{39}$$

$$\dot{v_{ij}} = -\sum_{\overline{ij}\in \mathrm{N}_{ij}} \eth_{ij,\overline{ij}}(v_{ij} - v_{\overline{ij}}) - B_{ij}\dot{x}_{ij} \tag{40}$$

$$\dot{\chi}_{e^p} = \Gamma_{\Omega_{e^p}}(\nabla^2 C(\chi_{e^p})^{-1}\chi_{e^p}, \nabla^2 C(\chi_{e^p})^{-1}(-\nabla C(\chi_{e^p}) + \lambda_{p,i} - \lambda_{p,k})) \tag{41}$$

$$\dot{\chi}_{e^h} = \Gamma_{\Omega_{e^h}}(\nabla^2 C(\chi_{e^h})^{-1}\chi_{e^h}, \nabla^2 C(\chi_{e^h})^{-1}(-\nabla C(\chi_{e^h}) + \lambda_{h,i} - \lambda_{h,k})) \tag{42}$$

$$\dot{\chi}_{e^g} = \Gamma_{\Omega_{e^g}}(\nabla^2 C(\chi_{e^g})^{-1}\chi_{e^h}, \nabla^2 C(\chi_{e^g})^{-1}(-\nabla C(\chi_{e^g}) + \lambda_{g,i} - \lambda_{g,k})) \tag{43}$$

$$\dot{\lambda}_{p,i} = -\left(\sum_{e_p=(i,k)} (\chi_{e^p}) - \sum_{e_p=(k,i)} (\chi_{e^p}) + (1+m_i)v_{i0}|_1\right) \tag{44}$$

Algorithm 1: DDND Algorithm.

Input : The parameters of $W(x_{ij})$, $C(\chi_{e^p})$, $C(\chi_{e^h})$, $C(\chi_{e^g})$, local operation constraints, node-edge incidence matrixes O^p, O^h and O^g.

Output : The final values of optimal energy generation and consumption as well as optimal energy exchange among EBs.

Initialize: Any admissible values for $x_{ij}(t_0) \in \Omega_{ij}$, $y_{ij}(t_0)$, $z_{ij}(t_0)$, $\chi_{e^p}(t_0) \in \Omega_{e^p}$, $\chi_{e^h}(t_0) \in \Omega_{e^h}$, $\chi_{e^g}(t_0) \in \Omega_{e^g}$, $\lambda_{p,i}(t_0)$, $\lambda_{h,i}(t_0)$, and $\lambda_{g,i}(t_0)$, and $v_{ij}(t_0) = -B_{ij}x_{ij}(t_0) + l_{ij}^m$.

```
repeat
  each participant and ER exchange the information of y_ij, z_ij and v_ij with its neighbors, and perform dynamics
    a) (37) to update x_ij;   b) (38) to update y_ij;
    c) (39) to update z_ij;   d) (40) to update v_ij.
  Each ER exchanges the information of λ_p,i, λ_h,i, λ_g,i with its neighbor ERs, and performs dynamics
    a) (41) to update χ_e^p;  b) (44) to update λ_p,i;
    c) (42) to update χ_e^h;  d) (45) to update λ_h,i;
    e) (43) to update χ_e^g;  f) (46) to update λ_g,i.
until Convergence;
```

$$\dot{\lambda}_{h,i} = -\left(\sum_{e_h=(i,k)} (\chi_{e^h}) - \sum_{e_h=(k,i)} (\chi_{e^h}) + (1+m_i) v_{i0}|_2 \right) \tag{45}$$

$$\dot{\lambda}_{g,i} = -\left(\sum_{e_g=(i,k)} (\chi_{e^g}) - \sum_{e_g=(k,i)} (\chi_{e^g}) + (1+m_i) v_{i0}|_3 \right). \tag{46}$$

where y_{ij}, z_{ij}, v_{ij}, $\lambda_{p,i}$, $\lambda_{h,i}$, and $\lambda_{g,i}$ are designed auxiliary variables, whose functionalities can be found in Appendix C in [32].

The implementation procedure of the proposed algorithm is summarized in Algorithm 1. It is worth noting that the Newton descent directions are embedded in the calculation of not only the optimal operation of each participant, i.e., (37), but also the optimal energy distribution on the edges among EBs, i.e., (41)–(43). For intuitive presentation, we name the above algorithm as DDND algorithm. The discretized implantation of the DDND algorithm is given in Appendix D in [32].

Remark 1: According to (41), besides the local information of $\nabla^2 C(\chi_{e^p})$ and $\nabla C(\chi_{e^p})$, the calculation of χ_{e^p} on the edge $e_p = (i,k)$ requires the information of $\lambda_{p,i}$ and $\lambda_{p,k}$. To calculate χ_{e^p}, we assign the computation task to the interconnected ER i and ER k by only letting ER i and ER k exchange information with each other. The same calculation method is applied to χ_{e^h} and χ_{e^g}. Meanwhile, the updating of $\lambda_{p,i}$, $\lambda_{h,i}$, and $\lambda_{g,i}$ is implemented through local computation as in (44)–(46). Then, each ER can calculate the exchanged energy with its neighbor ERs in a distributed fashion. Furthermore, in light of (37)–(40), the updating of variables x_{ij}, y_{ij}, z_{ij}, and v_{ij} only requires local information share and calculation. Thus, each participant can also find its optimal operations in a fully distributed fashion.

Remark 2: The existing algorithms (e.g., [5], [22]–[24], [26]–[29]) are not able to solve the studied problem of this article in a fully distributed manner. To be specific, the methods in [5], [22]–[24] do not consider the energy distribution constraints on interconnected lines, i.e., (35) and (36), which is only suitable for handling constraint (34). Note that (34)–(36) are different types of constraints, which cannot be simultaneously solved by the proposed distributed algorithms in [5], [22]–[24]. Next, the methods in [26]–[29] consider the constraint of power flow. However, they need to rely on coordinator(s) to management internal participants within individual microgrid or estimate part of global variables, which cannot be seen as fully distributed algorithms. Moreover, they do not consider the heat and gas networks as well as the strong coupling relationships among power, heat, and gas, which should be modeled in objective functions and constraints.

Next, the following Lemma 2 and Theorems 1 and 2 are further proposed to ensure the feasibility of the DDND algorithm in theory. To be specific, Lemma 2 gives the convergence property of dynamics (40) as follows.

Lemma 2: Suppose that graph G_i is connected and dynamics $\dot{x}_{ij}$ is stable. The initial points are chosen as $v_{ij}(t_0) = -B_{ij}x_{ij}(t_0) + l_{ij}^m$ and $x_{ij}(t_0) \in \Omega_{ij}$. Then, dynamics (40) makes

$$v_{ij}(t) \to -\frac{1}{1+m_i} \sum_{j=0}^{m_i} \left(x_{ij}(t) - l_{ij}^m \right), \quad t \to \infty. \tag{47}$$

The proof of Lemma 2 is presented in Appendix E in [32].

As assistant work, Lemma 1 (see Appendix B in [32]) and Lemma 2 are used for the convergence analysis of the subsequent main theoretical results. On these basis, the following Theorem 1 shows that the equilibrium point of the DDND algorithm is the optimal point and Theorem 2 further verifies the convergence of the DDND algorithm.

Theorem 1: Suppose that graphs $\mathcal{G}^p$, $\mathcal{G}^h$, $\mathcal{G}^g$, G, and G_i for $i = 1, \cdots, n$ are connected. Then, the equilibrium point of the DDND algorithm is the optimal solution of the studied problem i.e., (33)–(36).

The proof of Theorem 1 is presented in Appendix F in[32].

Theorem 2: Suppose that graphs $\mathcal{G}^p$, $\mathcal{G}^h$, $\mathcal{G}^g$, G, and G_i for $i = 1, \cdots, n$ are connected. Then, the DDND algorithm makes all variables exponentially converge to the optimal solutions of the studied problem, i.e., (33)–(36).

The proof of Theorem 1 is presented in Appendix G in[32].

In addition, note that the proposed DDND algorithm is suitable for solving common convex optimization with the form shown in (33)–(36). Thus, this algorithm can be expanded to solve more complicated model, if the system model can be relaxed as the form shown in (33)–(36).

Remark 3: It can be seen from Algorithm 1 that the variables to be communicated only include y_{ij}, z_{ij}, v_{ij}, $\lambda_{p,i}$, $\lambda_{h,i}$, and $\lambda_{g,i}$. Note that they are all floating-point numbers, each

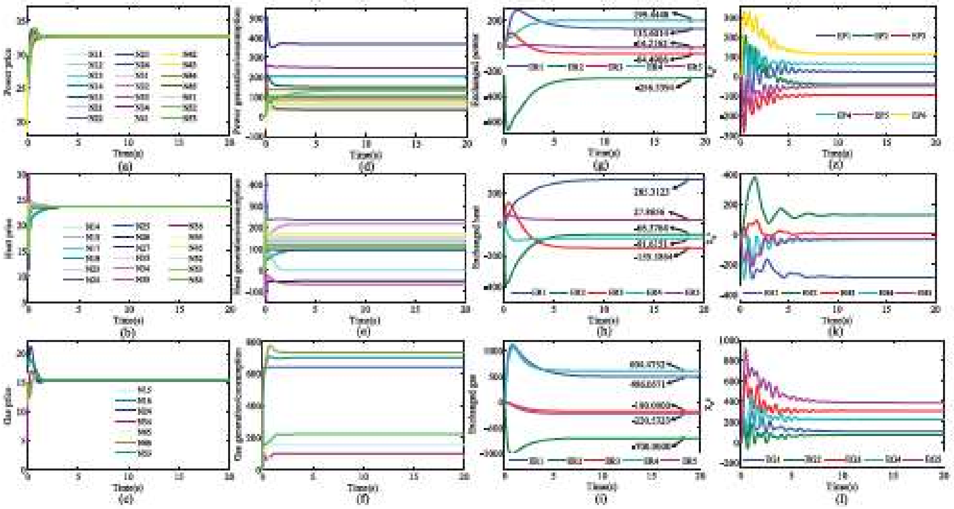

Fig. 2. Simulation results. (a) Power price. (b) Heat price. (c) Gas price. (d) Power generation/consumption. (e) Heat generation/consumption. (f) Gas generation/consumption. (g) Exchanged power. (h) Exchanged heat. (i) Exchanged gas. (j) Power distribution. (k) Heat distribution. (l) Gas distribution.

of which occupies 32-bits for single-precision or 64-bits for double-precision. For any pair of nodes (participant or ER), the amount of communication data (i.e., the total number of bits) is very small. Currently, most of the communication devices process the communication data transfer rate (CDTR) over the level of megabit per second, which is more than enough to meet the communication requirement for our considered problem. Additionally, in this article, each node only needs to share information with its neighbors in a short space distance, which does not involve the long-distance data transfer. Thus, the time delay for transmitting these numerical values is very short. Therefore, by using the currently advanced communication technology, there is negligible effect on our studied problem caused by the CDTR and the corresponding time delay.

Remark 4: In our proposed algorithm, the decision variables of each participant or ER only include its local variables but not the global variables. The computational complexity for individual participant or ER by implementing the proposed algorithm is $O(\varrho^3)$, where ϱ is the dimensionality of local variable. Note that ϱ is not changed with the system scale. Thus, the computational complexity for individual participant or ER is also not changed as the system scale.

Remark 5: The proposed algorithm possesses better robustness property against single and even several link failure(s), as long as the system or graph remains connected. The reasons are as follows. Since the connectivity is not broken, the corresponding graph Laplacian matrix remains symmetric, singular, and positive semidefinite. The graph Laplacian matrix, both before and after failure(s), holds one simple zero eigenvalue while the rest of eigenvalues are positive. Note that those properties are used for subsequent convergence proof. Since those properties are not changed, the convergence is not changed either.

IV. Simulation Results

Numerical simulations are presented to exhibit the performance of the proposed method for an EI system with five EBs. The system physical and communication structures are illustrated in Fig. A3(a) (see Appendix H in [32]), which are derived from [5]. The parameters of cost or utility functions as well as the local operation constraints of each participant are obtained from [5]. The cost parameters of the interconnected edges are listed in Table A1 (see Appendix H in[32]). The energy scales are unified as 1 p.u. = 1MW for power or heat, 1 p.u. = 84SCM/h for gas, and 1 p.u.=1MWh for price [22].

TABLE I
Termination Time

ACE	-4	-5	-6	-7	-8
DDND	16.9943s	18.2714s	20.3070s	22.6247s	24.9333s
DDGD	85.2326s	104.6773s	124.5019s	144.5963s	164.6294s
DNB	79.9825s	94.5893s	97.8965s	99.6548s	120.1546s

A. Convergence Analysis

In this case study, we aim to show the global optimality and convergence of the proposed DDND algorithm. The must-run electricity, heat, and gas loads for EB1 to EB5 are the same as those used by [5]. The initial directions of power exchange, heat exchange, and gas exchange across the interconnected edges among EBs are shown in Figs. A3(b)– A3(d) (see Appendix H in[32]). The simulation results by running the DDND algorithm are shown in Fig. 2. To be specific, Fig. 2(a)–(c) shows the estimated power, heat, and gas prices of each participant. It can be observed that, after approximately 10 s, the price of each type of energy converges to a common value which is the final market clearing price. Fig. 2(d)–(f) shows the trajectories of estimated power, heat, and gas generations/demands of each participant, whose final values are tabulated in Table A2 (see Appendix H in [32]). The results are almost the same as the ones corresponding to Table I in [5], which implies that each participant can locally obtain its optimal operation. Next, Fig. 2(g)–(i) shows the trajectories of the exchanged energy of each EB, i.e., $-(1+m_\imath)v_{\imath0}$, estimated by the corresponding ER. The final values are also marked in Fig. 2(g)–(i). It can be observed that

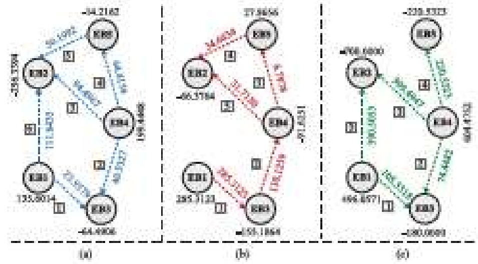

Fig. 3. Final energy trading layout. (a) Power trading layout. (b) Heat trading layout. (c) Gas trading layout.

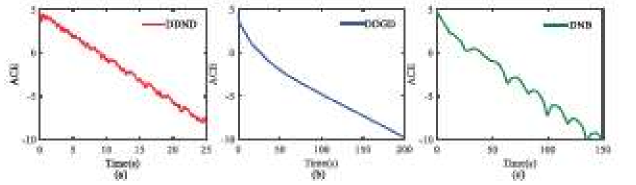

Fig. 4. Comparison results. (a) DDND algorithm. (b) DDGD algorithm. (c) DNB algorithm.

the estimated values are the same as the actual values shown in Table A2 (see Appendix H in [32]). Finally, Fig. 2(j)–(l) shows the energy distribution on interconnected lines among EBs. The final converged values are listed in Table A3 (see Appendix H in[32]). Note that some energy exchange values are negative, which means that the actual directions are opposite to the initial ones. For instance, the initial power exchange direction between EB3 and EB4, i.e., edge 2 shown in Fig. A2(b), is from EB3 to EB4. The calculation value is −40.5327(p.u.), which implies that the final direction is from EB4 to EB3. In other words, EB4 will sell 40.5327(p.u.) electricity power to EB3. To clearly see the energy trading layout, the final energy distribution on the interconnected lines as well as the exchanged energy of each EB are depicted in Fig. 3(a)–(c). It can be observed that, for each EB, the internal excess (or deficit) energy is equal to the amount of energy selling to (or buying from) its neighbors. Theses imply that the calculation results given by DDND algorithm are feasible and effective. Moreover, to further validate the optimality of the DDND algorithm, a classical centralized method, i.e., the PDIP algorithm [33], is used to calculate the optimal solutions of the same studied problem. The calculated results are listed in Tables A2 and A3 (see Appendix H in[32]). It can be observed that the calculated results obtained from our DDND algorithm and the PDIP algorithm are almost the same. Thus, this verifies that the proposed DDND algorithm can converge to the optimal solution.

B. Comparison Analysis

In this case study, we compare the Newton descent method with the gradient methods to show the faster convergence feature of the proposed DDND algorithm. Note that the existing distributed algorithms cannot directly solve the considered problem in a fully distributed fashion. To make a comparison with gradient descent method, we let all the Hessian matrices $\nabla^2 W(x_{ij})$, $\nabla^2 C(\chi_{e^p})$, $\nabla^2 C(\chi_{e^h})$, and $\nabla^2 C(\chi_{e^g})$ be set to the corresponding identity matrices. Then, the proposed DDND algorithm degenerates to a kind of gradient descent method which is referred to as distributed double-gradient descent (DDGD) algorithm. In addition, we also compare the proposed DDND algorithm with the distributed neurodynamic-based (DNB) algorithm regarding convergence speed. Therein, the DNB is proposed in [30] and applied to solve the EMP for integrated energy system in [25], recently. When the DNB algorithm is used to solve our studied problem, the global variables are required to be known by each participant and ER, leading to not fully distributed implementation. Next, to show the exponential convergence of the DDND algorithm in a better way, we define the averaged calculation error (ACE) in logarithmic scale, as follows:

$$\mathrm{ACE} = \ln\bigg(\frac{1}{\Im}\|X - X^{*}\| + \frac{1}{6}\|\chi^{p} - \chi^{p*}\| + \frac{1}{5}\|\chi^{h} - \chi^{h*}\| + \frac{1}{5}\|\chi^{g} - \chi^{g*}\|\bigg). \tag{48}$$

where X^{*}, $\chi^{P^{*}}$, $\chi^{h^{*}}$, and χ^{g*} are the optimal solutions of X, χ^{P}, χ^{h}, and χ^{g}, respectively. The total number of the ERs and participants, i.e., $\Im$ is equal to 36 for the test system shown in Fig. A3. In addition, the denominator values of 6, 5, and 5 in the second, third, and fourth items of the right hand of (48) are the numbers of total power lines, heat lines, and gas lines among EBs, respectively.

With the same setting of all the parameters, the trajectories of ACE by using the DDND algorithm, DDGD algorithm, and the DNB algorithm are shown in Fig. 4(a)–(c), respectively. To clearly see the results, we let each algorithm stop once ACE is below preset accuracy requirement; meanwhile, the corresponding computation time is recorded. The termination time under different values of ACE of the three algorithms are listed in Table I. It can be observed that the DDND algorithm requires less time than the DDGD algorithm and DNB algorithm to reach the same ACE. These results exhibit the faster convergence feature of the proposed DDND algorithm. This is because the DDND algorithm is able to take advantage of Newton descent information by using both second-order and first-order information to speed up the convergence.

C. One Day Energy Management

In this case study, we test the performance of the proposed algorithm for one day energy management with changing renewable generations and load demands. The forecasting renewable energy generation and must-run energy load variations for one day are shown in Fig. 5(a)–(c). Therein, PL, HL, and GL represent the must-run power, heat, and gas loads, respectively. The system structure and parameters are the same as the first case study. By implementing the proposed DDND algorithm, the profiles of power, heat, and gas generations/demands are presented in Fig. 5(d)–(f). Meanwhile, the profiles of energy flow distributions on the interconnected lines among EBs are presented in Fig. 5(g)–(i). It should be pointed out that, for each hour's dispatch period, the algorithm converges in less than 20 s. It can be seen that the proposed algorithm can automatically respond to the variations of the renewable energy generations and load demands, and converge to new state during each dispatch

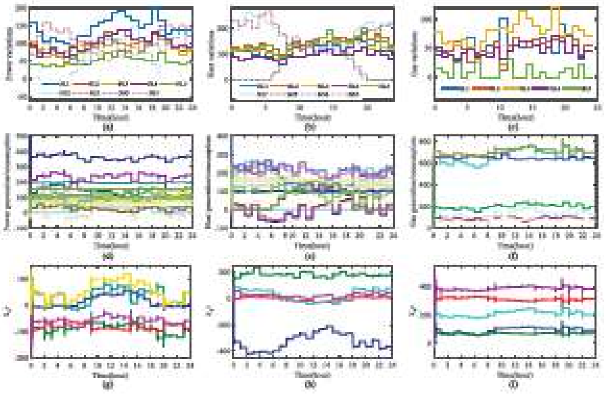

Fig. 5. Simulation results for one-day scenario. (a) Renewable power generation or must-run power load variations. (b) Renewable heat generation or must-run heat load variations. (c) Must-run gas load variations. (d) Power generation/consumption. (e) Heat generation/consumption. (f) Gas generation/consumption. (g) Power distribution. (h) Heat distribution. (i) Gas distribution.

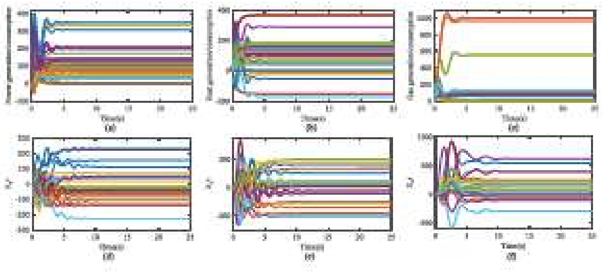

Fig. 6. Simulation in large-scale system. (a) Power generation/consumption. (b) Heat generation/consumption. (c) Gas generation/consumption. (d) Power distribution. (e) Heat distribution. (f) Gas distribution.

period. It implies that the proposed DDND algorithm possesses better adaptivity and robustness with changing system operating conditions.

D. Effectiveness Analysis in a Large-Scale Test System

In this case study, we focus on analyzing the effectiveness of the proposed algorithm in a large-scale test system. The system physical structure of the large-scale text system is shown in Fig. A4 (see Appendix H in [32]). Without loss of generality, we let the communication network overlays the physical network. The parameters for each type of participant are similar to those in [22]. The parameters for each type of interconnected line are similar to those in Table A1. We randomly set the initial flow directions of power exchange, heat exchange, and gas exchange across the interconnected edges among EBs. The trajectories of estimated power, heat, and gas generations/demands of each participant are shown in Fig. 6(a)–(c). The energy flow distributions on the interconnected lines among EBs are shown in Fig. 6(d)–(f). It can be observed that all those decision variables converge after approximately 15 s. Compared with the results in the first case study, although the system scale has tripled in size approximatively, the convergence time has not increased significantly. This result shows that the fast convergence speed is still ensured in the large-scale system, which further verifies the effectiveness of the proposed DDND algorithm.

V. Conclusion

In this article, to achieve the cooperative energy management of multiple distributed energy networks in the processes of energy generation, delivery, and consumption, a multiobjective energy management model was built within the context of EB-based EI. It was further formulated as a distributed optimization problem with multiple equality and inequality constraints. By primal-dual analysis and Taylor expansion, a DDND algorithm was further proposed to solve such kind of optimization problem with some satisfactory features including fully distributed execution as well as faster convergence speed. By using Lyapunov stability theory, we proved that the proposed DDND algorithm was able to converge to the global optimal solution. In future work, we will consider more complex system model and study effective relaxation approach to further expand the application of the DDND algorithm.

References

[1] H. Guo, F. Wang, L. Li, L. Zhang, and J. Luo, "A minimum loss routing algorithm based on real-time transaction in energy internet," *IEEE Trans. Ind. Informat.*, vol. 15, no. 12, pp. 6446–6456, Dec. 2019.

[2] H. Hua, Y. Qin, C. Hao, and J. Cao, "Stochastic optimal control for energy Internet: A bottom-up energy management approach," *IEEE Trans. Ind. Informat.*, vol. 15, no. 3, pp. 1788–1797, Mar. 2019.

[3] H. Hua, Y. Qin, and C. Hao *et al.*, "Optimal energy management strategies for energy Internet via deep reinforcement learning approach," *Appl. Energy*, vol. 239, pp. 598–609, 2019.

[4] R. Wang, S. Qiuye, M. Dazhong, and H. Xuguang, "Line impedance cooperative stability region identification method for grid-tied inverters under weak grids," *IEEE Trans. Smart Grid*, vol. 11, no. 4, pp. 2856–2866, Jul. 2020, doi: 10.1109/TSG.2020.2970174.

[5] H. Zhang, Y. Li, D. W. Gao, and J. Zhou, "Distributed optimal energy management for energy internet," *IEEE Trans. Ind. Informat.*, vol. 13, no. 6, pp. 3081–3097, Dec. 2017.

[6] H. Xing, Y. Mou, M. Fu, and Z. Lin, "Distributed bisection method for economic power dispatch in smart grid," *IEEE Trans. Powers Syst.*, vol. 30, no. 6, pp. 3024–3035, Nov. 2015.

[7] G. Binetti, A. Davoudi, F. L. Lewis, D. Naso, and B. Turchiano, "Distributed consensus-based economic dispatch with transmission losses," *IEEE Trans. Powers Syst.*, vol. 29, no. 4, pp. 1711–1720, Jul. 2014.

[8] F. D. Kanellos, E.-S. M. Volanis, and N. Hatziargyriou, "Power management method for large ports with multi-agent systems," *IEEE Trans. Smart Grid*, vol. 10, no. 2, pp. 1259–1268, Mar. 2019.

[9] J. Zhou, Y. Xu, H. Sun, Y. Li, and M. Chow, "Distributed power management for networked AC/DC microgrids with unbalanced microgrids," *IEEE Trans. Ind. Informat.*, vol. 16, no. 3, pp. 1655–1667, Mar. 2020.

[10] J. Zhou, Y. Xu, H. Sun, L. Wang, and M. -Y. Chow, "Distributed event-triggered H_∞ consensus based current sharing control of DC microgrids considering uncertainties," *IEEE Trans. Ind. Informat.*, vol. 16, no. 12, pp. 7413–7425, Dec. 2020, doi: 10.1109/TII.2019.2961151.

[11] Z. Zhang and M.-Y. Chow, "Convergence analysis of the incremental cost consensus algorithm under different communication network topologies in a smart grid," *IEEE Trans. Powers Syst.*, vol. 27, no. 4, pp. 1761–1768, Nov. 2012.

[12] S. Yang, S. Tan, and J. Xu, "Consensus based approach for economic dispatch problem in a smart grid," *IEEE Trans. Powers Syst.*, vol. 28, no. 4, pp. 4416–4426, Nov. 2013.

[13] Y. Xu and Z. Li, "Distributed optimal resource management based on the consensus algorithm in a microgrid," *IEEE Trans. Ind. Electron.*, vol. 62, no. 4, pp. 2584–2592, Apr. 2015.

[14] G. Chen and Z. Zhao, "Delay effects on consensus-based distributed economic dispatch algorithm in microgrid," *IEEE Trans. Power Syst.*, vol. 33, no. 1, pp. 602–612, Jan. 2018.

[15] B. Huang, L. Liu, H. Zhang, Y. Li, and Q. Sun, "Distributed optimal economic dispatch for microgrids considering communication delays," *IEEE Trans. Syst., Man, Cybern., Syst.*, vol. 49, no. 8, pp. 1634–1642, Aug. 2019.

[16] F. Li, J. Qin, Y. Kang, and W. X. Zheng, "Consensus based distributed reinforcement learning for nonconvex economic power dispatch in microgrids," *in Neural Inf. Process.* (Series Lecture Notes in Computer Science). Berlin, Germany: Springer, Nov. 2017, pp. 831–839.

[17] F. Li, J. Qin, and Y. Kang, "Multi-agent system based distributed pattern search algorithm for non-convex economic load dispatch in smart grid," *IEEE Trans. Power Syst.*, vol. 34, no. 3, pp. 2093–2102, May 2019.

[18] Q. Li, D. W. Gao, H. Zhang, Z. Wu, and F. Wang, "Consensus-based distributed economic dispatch control method in power systems," *IEEE Trans. Smart Grid*, vol. 10, no. 1, pp. 941–954, Jan. 2019.

[19] Y. Jia, Z. Y. Dong, C. Sun, and K. Meng, "Cooperation-based distributed economic MPC for economic load dispatch and load frequency control of interconnected power systems," *IEEE Trans. Power Syst.*, vol. 34, no. 5, pp. 3964–3966, Sep. 2019, doi: 10.1109/TPWRS.2019.2917632.

[20] P. Li, Y. Liu, H. Xin, and X. Jiang, "A robust distributed economic dispatch strategy of virtual power plant under cyber-attacks," *IEEE Trans. Ind. Informat.*, vol. 14, no. 10, pp. 4343–4352, Oct. 2018.

[21] J. Duan and M. Chow, "A novel data integrity attack on consensus-based distributed energy management algorithm using local information," *IEEE Trans. Ind. Informat.*, vol. 15, no. 3, pp. 1544–1553, Mar. 2019.

[22] Y. Li, H. Zhang, X. Liang, and B. Huang, "Event-triggered based distributed cooperative energy management for multi-energy systems," *IEEE Trans. Ind. Informat.*, vol. 15, no. 14, pp. 2008–2022, Apr. 2019.

[23] Q. Sun, R. Fan, Y. Li, B. Huang, and D. Ma, "A distributed double-consensus algorithm for residential We-Energy," *IEEE Trans. Ind. Informat.*, vol. 15, no. 8, pp. 4830–4842, Aug. 2019.

[24] X. Le, S. Chen, F. Li, Z. Yan, and J. Xi, "Distributed neurodynamic optimization for energy internet management," *IEEE Trans. Syst., Man, Cybern., Syst.*, vol. 49, no. 8, pp. 1624–1633, Aug. 2019, doi: 10.1109/TSMC.2019.2898551.

[25] Z. Yi, Y. Xu, J. Hu, M. Chow, and H. Sun, "Distributed neurodynamic-based approach for economic dispatch in an integrated energy system," *IEEE Trans. Ind. Informat.*, vol. 16, no. 4, pp. 2245–2257, Apr. 2020.

[26] T. Xu, W. Wu, and H. Sun *et al.*, "Fully distributed multi-area dynamic economic dispatch method with second-order convergence for active distribution networks," *IET Gener. Transmiss. Distrib.*, vol. 11, no. 16, pp. 3955–3965, 2017.

[27] T. Xu, W. Wu, W. Zheng, H. Sun, and L. Wang, "Fully distributed quasi-Newton multi-area dynamic economic dispatch method for active distribution networks," *IEEE Trans. Power Syst.*, vol. 33, no. 4 pp. 4253–4263, Jul. 2018.

[28] Y. Liu *et al.*, "Distributed robust energy management of a multimicrogrid system in the real-time energy market," *IEEE Trans. Sustain. Energy*, vol. 10, no. 1, pp. 396–406, Jan. 2019.

[29] J. Ahmad, M. Tahir, and S. Mazumder, "Improved dynamic performance and hierarchical energy management of microgrids with energy routing," *IEEE Trans. Ind. Informat.*, vol. 15, no. 8, pp. 3218–3229, Jun. 2019.

[30] Q. Liu, S. Yang, and J. Wang, "A collective neurodynamic approach to distributed constrained optimization," *IEEE Trans. Neural Netw. Learn. Syst.*, vol. 28, no. 8, pp. 1747–1758, Aug. 2017.

[31] Y. Xu, W. Wu, and J. Zhou, "A distributed task allocation based on a winner-take-all approach for multiple energy storage systems coordination in a microgrid," *IEEE Trans. Smart Grid*, vol. 11, no. 1, pp. 686–695, Jan. 2020.

[32] 2020. [Online]. Available: https://www.researchgate.net/publication/344467333_Appendixes

[33] AsdS. Wright, *Primal-Dual Interior-Point Methods*. Philadelphia, PA, USA: SIAM, 1997.

Yushuai Li (Member, IEEE) received the B.S. degree in electrical engineering and automation, and the Ph.D. degree in control theory and control engineering from Northeastern University, Shenyang, China, in 2014 and 2019, respectively.

From 2019 to 2020, he was a Postdoctoral Research Scholar with the Department of Electrical and Computer Engineering, University of Denver, Denver, CO, USA. He is currently a Lecturer with the School of Information Science and Engineering, Northeastern University, Shenyang, China. He serves as a Guest Editor for the Complexity on the Special Issue "*Theory and Applications of Cyber-Physical Systems.*" His main research interests include distributed modeling, control, energy management and optimization of energy Internet and multienergy systems, as well as distributed machine learning algorithm with applications in microgrids.

David Wenzhong Gao (Senior Member, IEEE) received the M.S. and Ph.D. degrees in electrical and computer engineering, specializing in electric power engineering, from Georgia Institute of Technology, Atlanta, GA, USA, in 1999 and 2002, respectively.

He is currently with the Department of Electrical and Computer Engineering, University of Denver, Denver, CO, USA. His current teaching and research interests include renewable energy and distributed generation, microgrid, smart grid, power system protection, power electronics applications in power systems, power system modeling and simulation, and hybrid electric propulsion systems.

Dr. Gao is an Associate Editor for the IEEE JOURNAL OF EMERGING AND SELECTED TOPICS IN POWER ELECTRONICS, and *Journal of Modern Power Systems and Clean Energy*. He was an Editor of the IEEE TRANSACTIONS ON SUSTAINABLE ENERGY. He is the General Chair for the 48th North American Power Symposium (NAPS 2016) and the IEEE Symposium on Power Electronics and Machines in Wind Applications (PEMWA 2012).

Wei Gao (Graduate Student Member) received the bachelor's degree in automation from the Hebei University of Technology, Tianjin, China, in 2017. He is currently working toward the Ph.D. degree with the Department of Electrical and Computer Engineering, University of Denver, Denver, CO, USA.

His current research interests are microgrid control, renewable energy, and power system stability.

Huaguang Zhang (Fellow, IEEE) received the B.S. and M.S. degrees in control engineering from Northeast Dianli University of China, Jilin, China, in 1982 and 1985, respectively, and the Ph.D. degree in thermal power engineering and automation from Southeast University, Nanjing, China, in 1991.

He was with the Department of Automatic Control, Northeastern University, Shenyang, China, in 1992, as a Postdoctoral Fellow for two years. Since 1994, he has been a Professor and Head of the Institute of Electric Automation, School of Information Science and Engineering, Northeastern University, Shenyang, China. He has authored and coauthored more than 280 journal and conference papers, six monographs, and co-invented 90 patents. His main research interests are fuzzy control, stochastic system control, neural networks based control, nonlinear control, and their applications.

Dr. Zhang is the E-letter Chair of IEEE CIS Society, the former Chair of the Adaptive Dynamic Programming & Reinforcement Learning Technical Committee on IEEE Computational Intelligence Society. He is an Associate Editor of *Automatica*, IEEE TRANSACTIONS ON NEURAL NETWORKS, IEEE TRANSACTIONS ON CYBERNETICS, and *Neurocomputing*. He was an Associate Editor for the IEEE TRANSACTIONS ON FUZZY SYSTEMS (2008–2013). He was the recipient of the Outstanding Youth Science Foundation Award from the National Natural Science Foundation Committee of China in 2003. He was named the Cheung Kong Scholar by the Education Ministry of China in 2005. He was also the recipient of the IEEE Transactions on Neural Networks 2012 Outstanding Paper Award.

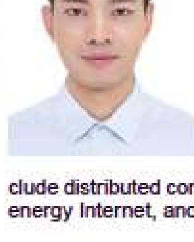

Jianguo Zhou (Member, IEEE) received the B.S. degree in automation and the M.S. and Ph.D. degrees in control theory and control engineering from Northeastern University, Shenyang, China, in 2011, 2013, and 2018, respectively.

Since 2018, he has been a Postdoctoral Researcher with the Tsinghua-Berkeley Shenzhen Institute, Tsinghua Shenzhen International Graduate School, Tsinghua University, Shenzhen, China. His current research interests include distributed control and optimization with applications in microgrids, energy Internet, and integrated energy systems.